Electronic Supplementary Material (ESI) for Catalysis Science & Technology.


# Contents

1 Experimental ..... 2
1.1 Autoclave Reactions ..... 2
1.2 GC/LC Analysis ..... 2
1.3 Activation Energy ..... 2
2 Stereoisomerization ..... 2
2.1 Stereoisomerization of Xylitol ..... 3
2.2 Stereoisomerization of Sorbitol ..... 3
3 Simultaneous Deoxygenation and Decarbonylation of Xylitol (model 2) ..... 4
4 Consecutive Decarbonylation ..... 5
4.1 Decarbonylation of pentitols ..... 5
4.2 Decarbonylation of Hexitols ..... 5

# 1 Experimental

Ru/C (5 wt%), tungstosilicic acid hydrate, allitol, D-talitol, L-iditol and L-rhamnose monohydrate (>99%) were obtained from Sigma-Aldrich. D(-)-Sorbitol (molecular Biology grade) was obtained from AppliChem. Galactitol, D(+)-arabitol, mannitol, D-ribitol, xylitol and erythritol were obtained from Supelco.

## 1.1 Autoclave Reactions

Experiments were performed in a 50 mL batch-type high-pressure autoclave reactor. Typically, substrate (2.0 g) and Ru/C (0.4 g) were added into a glass-lined stainless steel reactor equipped with a sampling valve and charged with $H_2O$ (20 mL). The reactor was flushed several times with 6 MPa $H_2$ at room temperature. The reactor was pressurized with 6 MPa $H_2$ and then heated to the defined temperature (393–443 K). The time zero was set 20-30 min after the beginning of the isothermal reaction stage.

## 1.2 GC/LC Analysis

0.5 mL aliquots were dried using a Eppendorf Speedvac system (303 K, 8 h). The resulting residue was dissolved in 1 mL acetic anhydride/pyridine mixture (1:1 v/v) and left to react for 3 days at room temperature with periodic mixing and shaking. Subsequently the sample solutions were measured by GC (Thermo Scientific Trace GC system with an Agilent DB-23 column (i.d.: 0.25 mm, length: 60 m, film thickness: 0.25 µm, Isobaric: 0.1 MPa He, temperature gradient: 353–527 K) or a CP-SIL PONA CB column (i.d.: 0.21 mm, length: 50 m, film thickness: 0.21 µm, isobaric: 0.1 MPa He, temperature gradient: 323–503 K)), GC-MS (Thermo Scientific Trace 1310 system equipped with a single quadrupole MS, EI+, 70 eV) and/or HPLC-ESI-MS (Shimadzu LC-MS 2020 system with a LiChrospher 100 column (RP-18e, length: 25 cm, particle size: 5 µm, binary gradient 30–50 %B (A: 10 mM ammonium acetate aqueous soln. with 0.1% formic acid, B: acetonitrile (0.1% formic acid))). All compounds were calibrated using the external standard method. Isomeric products were treated as possessing equal response factors. Hexitols were calibrated using sorbitol. The pentitols were calibrated using xylitol. The tetritols were calibrated using erythritol. The hydrogenated solution of L-rhamnose was used to quantify hexanepentaols.

## 1.3 Activation Energy

Apparent activation energies ($\Delta H^{\ddagger}$) were determined by linear regression of ln(k/T) vs 1/T in accordance with the linearized form of the Eyring-Polanyi equation (Eq. 1).

$$\ln\frac{k}{T} = \frac{-\Delta H^{\ddagger}}{R}\cdot\frac{1}{T} + \ln\frac{k_B}{h} + \frac{\Delta S^{\ddagger}}{R} \qquad (1)$$

# 2 Stereoisomerization

Model concentrations based on eq. 1 – 9 were calculated numerically (1 min interval) and experimental data were fitted using the least squares method by variation of the rate constants (MS Excel solver add-in, GRG non-linear). Using this approach good fits were obtained in all cases, however, the obtained rate constants showed a very wide distribution (i.e., in some cases the values were unrealistically high or low). In addition, restarting the optimization from the same initial state led to different solutions. The

fact that 6 rate constants (or 16) are required to describe the evolution of only 3 (or 6) components means that these systems are inherently underdetermined. As a result the reliability of a specific solution is questionable. Regardless, the rate constants of XYL to ARA ($k_{xa}$) and RIB ($k_{xr}$) and SOR to MAN ($k_{sm}$), ALL ($k_{sa}$) GAL ($k_{sg}$) and IDI ($k_{si}$) showed only a low variance. This is rationalized by considering that starting from XYL and SOR the evolution of models is initially controlled by these rate constants. The importance of the other rate constants gradually increases as the system approaches equilibrium. Given that these epimerization reactions all follow the same mechanism, it can be assumed that the activation barriers and hence the rates are also comparable (i.e. albeit with subtle differences). Thus it can be postulated that the rate constants should be approximately equal and that large deviations are likely an error. A constraint was added to the model to dampen these errors. The difference between a rate constant $k_i$ and the average rate constant $k_{avg}$ was treated as a residual. In a second iterative step the product of the sums of the model and rate residuals was minimized. The fit was not noticeably affected by this. Due to the aforementioned issues with the model it was decided than only the most reliable rate constants would be considered for the determination of activation energies.

## 2.1 Stereoisomerization of Xylitol

$$\frac{dC_x}{dt} = -C_x \cdot k_{xa} - C_x \cdot k_{xr} + C_a \cdot k_{ax} + C_r \cdot k_{rx} \quad (2)$$

$$\frac{dC_a}{dt} = -C_a \cdot k_{ax} - C_a \cdot k_{ar} + C_x \cdot k_{xa} + C_r \cdot k_{ra} \quad (3)$$

$$\frac{dC_r}{dt} = -C_r \cdot k_{ra} - C_r \cdot k_{rx} + C_a \cdot k_{ra} + C_x \cdot k_{xr} \quad (4)$$

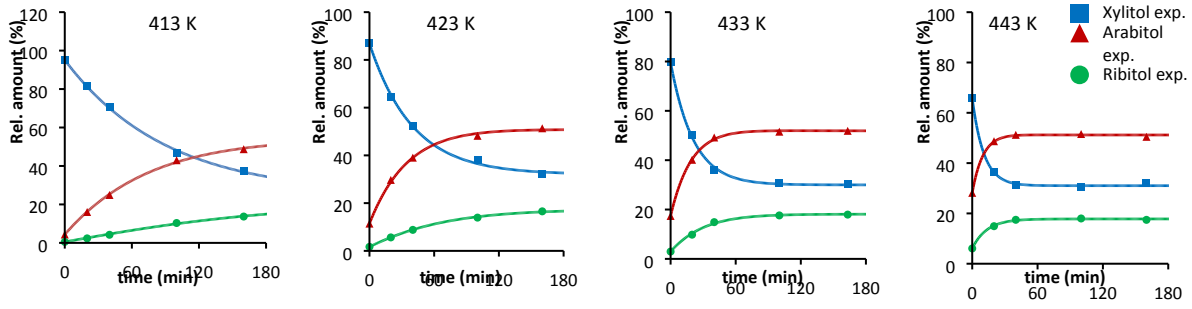


**Figure S1.** Ru/C-catalysed stereoisomerization of xylitol. (conditions: 2 g xylitol, 20 ml $H_2O$, 0.4 g Ru/C (5wt%), 6 MPa $H_2$).

## 2.2 Stereoisomerization of Sorbitol

$$\frac{dC_s}{dt} = -C_s \cdot k_{sm} - C_s \cdot k_{sa} - C_s \cdot k_{sg} - C_s \cdot k_{si} + C_m \cdot k_{ms} + C_a \cdot k_{as} + C_g \cdot k_{gs} + C_i \cdot k_{is} \quad (5)$$

$$\frac{dC_m}{dt} = -C_m \cdot k_{ms} - C_m \cdot k_{mt} + C_s \cdot k_{sm} + C_t \cdot k_{tm} \quad (6)$$

$$\frac{dC_a}{dt} = -C_a \cdot k_{as} - C_a \cdot k_{at} + C_s \cdot k_{sa} + C_t \cdot k_{ta} \quad (7)$$

$$\frac{dC_g}{dt} = -C_g \cdot k_{gs} - C_g \cdot k_{gt} + C_s \cdot k_{sg} + C_t \cdot k_{tg} \quad (8)$$

$$\frac{dC_i}{dt} = -C_i \cdot k_{is} - C_i \cdot k_{it} + C_s \cdot k_{si} + C_t \cdot k_{ti} \quad (9)$$

$$\frac{dC_t}{dt} = -C_t \cdot k_{tm} - C_t \cdot k_{ta} - C_t \cdot k_{tg} - C_t \cdot k_{ti} + C_m \cdot k_{mt} + C_a \cdot k_{at} + C_g \cdot k_{gt} + C_i \cdot k_{it} \quad (10)$$

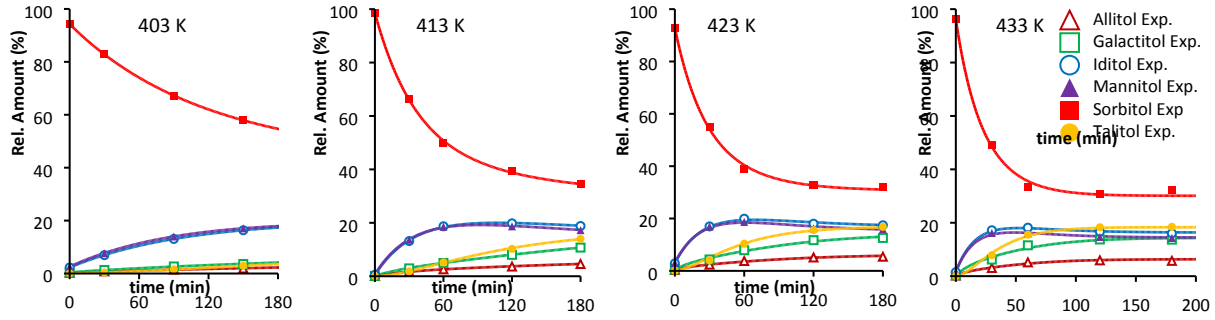


**Figure S2**. Ru/C-catalyzed stereoisomerization of sorbitol. (conditions: 2 g sorbitol, 20 ml $H_2O$, 0.4 g Ru/C (5wt%), 6 MPa $H_2$).

# 3 Simultaneous Deoxygenation and Decarbonylation of Xylitol (model 2)

$$\frac{dC_p}{dt} = -C_p \cdot k_{pt} - C_p \cdot k_{54} - C_p \cdot k_{wp} \quad (11)$$

$$\frac{dC_t}{dt} = -C_t \cdot k_{wt} + C_p \cdot k_{pt} \quad (12)$$

$$\frac{dC_{54}}{dt} = -C_{54} \cdot k_{w4} + C_p \cdot k_{54} \quad (13)$$

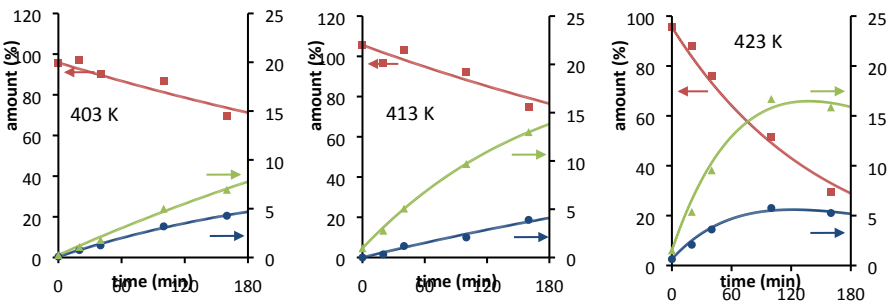

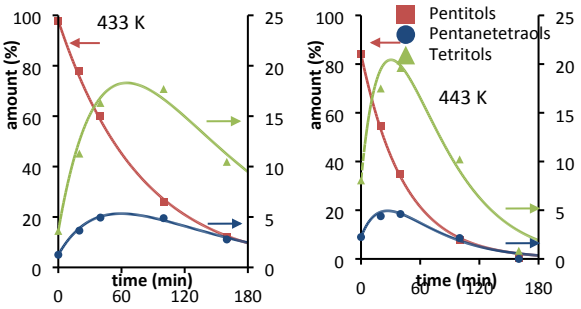


**Figure S3**. Modelling Ru/C-catalyzed simultaneous decarbonylation and deoxygenation of xylitol (model 2). (conditions: 2 g xylitol, 20 ml $H_2O$, 0.4 g Ru/C (5wt%), 6 MPa $H_2$).

# 4 Consecutive Decarbonylation

$$\frac{dC_h}{dt} = -C_h \cdot k_{hp} - C_h \cdot k_{wh} \quad (14)$$

$$\frac{dC_p}{dt} = -C_p \cdot k_{pt} - C_p \cdot k_{wp} + C_h \cdot k_{hp} \quad (15)$$

$$\frac{dC_t}{dt} = -C_t \cdot k_{tg} - C_t \cdot k_{wt} + C_p \cdot k_{pt} \quad (16)$$

$$\frac{dC_g}{dt} = -C_g \cdot k_{ge} - C_g \cdot k_{wg} + C_t \cdot k_{tg} \quad (17)$$

$$\frac{dC_e}{dt} = -C_e \cdot k_{we} + C_g \cdot k_{ge} \quad (18)$$

## 4.1 Decarbonylation of pentitols

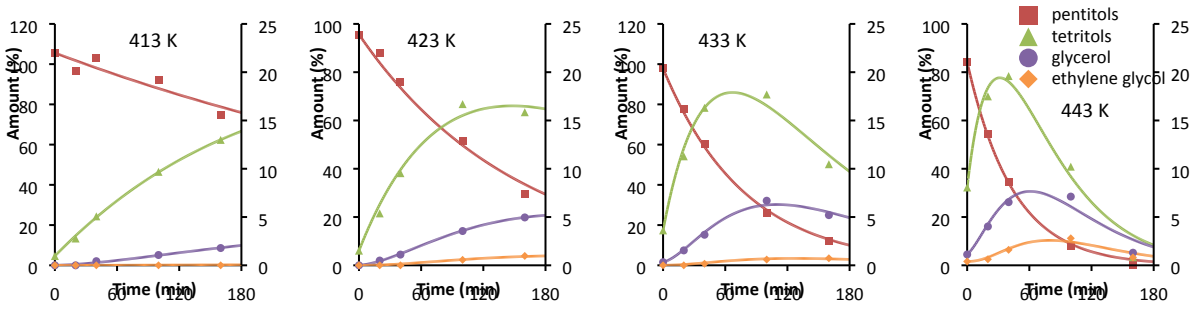


**Figure S4**. Modelling Ru/C-catalyzed consecutive decarbonylation of xylitol. (conditions: 2 g xylitol, 20 mL $H_2O$, 0.4 g Ru/C (5wt%), 6 MPa $H_2$).

## 4.2 Decarbonylation of Hexitols

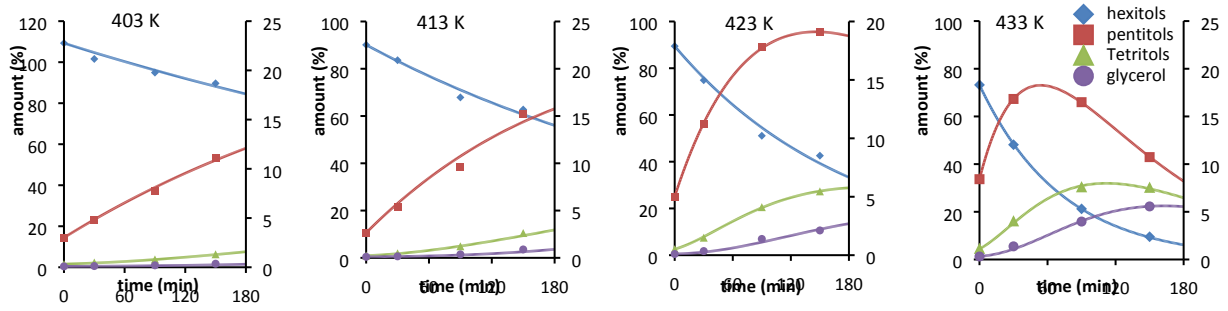


**Figure S5**. Modelling Ru/C-catalyzed consecutive decarbonylation of sorbitol. (conditions: 2 g sorbitol, 20 mL $H_2O$, 0.4 g Ru/C (5wt%), 6 MPa $H_2$).